OCEAN APPLICATIONS TECHNICAL NOTE 22

Assessment of a Global Data Assimilation System for Real-Time Ocean Forecasting

by

Michael J. Bell, Richard M. Forbes and Adrian Hines

Met Office
FitzRoy Road, Exeter, Devon. EX1 3PB

1. Introduction

The prospects for routine monitoring of the state of the ocean have improved dramatically over the last decade. The ocean is now more widely observed than ever before by a range of satellite-based instruments and programs of voluntary and dedicated *in situ* measurements (Busalacchi 1997). Recent technological advances have led to proposals (Argo Science Team 1998) to make further dramatic improvements to the *in situ* observing system. Furthermore, the increase in computing power has encouraged the development of complex numerical models to simulate the ocean circulation, whilst improvements in numerical weather prediction models have given access to surface fluxes with high temporal resolution of sufficient quality for use in forcing ocean models (World Climate Research Programme 1996).

There are now a number of systems in place for analysing and forecasting the upper layers of the open ocean in near real-time. In particular, the U.S. Navy's Ocean Thermal Information System, OTIS, (Clancy et al. 1992) has produced daily global analyses of the ocean's thermal structure for a number of years and the Australian Bureau of Meteorology Research Centre (BMRC) has also produced subsurface thermal analyses on a routine basis since 1988 (Smith 1995). Numerical ocean model based systems which assimilate oceanographic data on a regular basis have been developed by US National Center for Environmental Prediction (NCEP) (Ji et al. 1995, Behringer et al. 1998) and Kimoto et al. (1997). Many of the near real-time systems have focused on the tropical Pacific Ocean as this is the centre of activity for the El Niño-Southern Oscillation (ENSO) and is relatively well observed with *in situ* data from the TOGA-TAO array of moored buoys (Hayes et al., 1991). A few systems have been developed for prediction of mesoscale motions at higher latitudes including the French SOAP model (Dombrowsky and de Mey 1992) producing forecasts for the Azores frontal region, the relocatable Harvard Ocean Prediction System (HOPS, Robinson et al. 1996), and a Pacific Ocean system for operational use at the U.S. Fleet Numerical Meteorological and Oceanographic Centre (FNMOC) (Smedstad et al. 1997).

A global ocean analysis and forecasting system has been implemented at the U.K. Meteorological Office (UKMO) to provide routine daily analyses and short term forecasts for the Royal Navy. Known as the Forecasting Ocean Atmosphere Model (FOAM), the system is based on a 1° resolution primitive equation model of the global ocean and a data assimilation scheme for thermal profile and sea surface temperature observations. The objectives of this paper are to describe the FOAM data assimilation system and to determine the extent to which the assimilation scheme can compensate for errors in the model and surface forcing fluxes. Details of the ocean model, the assimilation scheme and the observation quality control are described in Section 2. The performance of the assimilation scheme is assessed with a series of one year integrations of the FOAM system and Section 3 presents results from the integrations with verification against independent observations and gridded climatological temperature fields. A discussion follows in Section 4 and the final section provides a concluding summary and describes plans for future enhancements to the system.

2. The FOAM assimilation and forecast system

a. Ocean and ice models

The ocean model is a component of the UKMO Unified Model System (Cullen 1993) and is based on the Cox (1984) formulation of the discretised primitive equations (Bryan 1969).

The model is used in coupled ocean-atmosphere climate simulations (Johns et al. 1997), for seasonal forecasting (Davey et al. 1994) and for the short-term ocean forecasting application (FOAM) described in this paper. FOAM uses a global version of the ocean model with a 1° resolution grid, 20 layers in the vertical and a timestep of 1 hour. Model levels are unevenly spaced with the vertical resolution decreasing with depth, from 10 metres near the surface to 600 metres in the deep ocean. The model bathymetry is derived from the DBDB5 dataset (U. S. Naval Oceanographic Office 1983) by interpolating onto the 1° global grid and smoothing by two applications of a 2D 1-4-1 type filter to remove large bathymetric gradients. In addition some channels have been widened or deepened as in Johns et al. (1997). The model includes a rigid-lid approximation and the velocity is represented by a baroclinic component and a barotropic streamfunction. Tracer advection is calculated using a centred difference leapfrog scheme; momentum fluxes are as described in section 8 of Bell (1998) for experiment D sm2. Fourier filtering is applied to the tracer and velocity fields north of 75°N.

Horizontal and vertical mixing on the sub-grid scale are parameterised in the model. The Richardson number dependent vertical diffusion scheme of Pacanowski and Philander (1981) is applied to mix temperature, salinity and horizontal momentum (using the coefficients they recommend). An additional mixed layer scheme based on Kraus and Turner (1967) and Davis et al. (1981) is used to mix the tracers (70% of the wind mixing energy is taken to be available for turbulent mixing and this is taken to decay exponentially with a depth scale of 100 m; 15% of convectively generated turbulent kinetic energy is taken to be available for entrainment at the base of the mixed layer). A simple version of the Large et al. (1994) scheme also mixes horizontal momentum in the vertical. For this a quadratic mixing profile (appropriate in neutral stability conditions) is used. The base of the mixing layer is set at the depth where the Richardson number first exceeds the critical value of 0.3, but is limited to be no deeper than 140 metres. The diffusion coefficient is chosen to match the Pacanowski and Philander value at this depth. Lateral mixing of tracers follows the method of Redi (1982) as amended by Gerdes et al. (1991) with a value of 2000 m^2s^{-2} at the surface decreasing to 500 m^2s^{-2} over a depth scale of 500 m and reduced where isopycnal slopes are greater than 1 in 1000. There is also a small amount of horizontal mixing (100 m^2s^{-1}) which is necessary to control grid scale noise. The horizontal viscosity is set to 6000 m^2s^{-2}.

The temperature of the top layer of the ocean model is relaxed towards a temperature climatology (as suggested by Haney 1971) with a relaxation coefficient of 35 $Wm^{-2}K^{-2}$. The surface salinity is also relaxed to climatology. The Levitus (1994) climatology is used for both temperature and salinity and sea ice thickness is relaxed to a climatology derived from the 2nd coupled version of the Unified Model (Johns et al. 1997). Both climatological and Numerical Weather Prediction (NWP) derived estimates of surface forcing fluxes are available to drive the ocean model. The monthly mean climatologies used in the integrations described in this paper were heat (Oberhuber 1988), wind stress (Hellerman and Rosenstein 1983), evaporation (Esbensen and Kushnir 1981) and precipitation (Jaeger 1983). Surface forcing fields derived from the global NWP model analysis are produced operationally four times a day at the UKMO. The operational version of FOAM is forced with these 6- hourly mean fluxes but monthly averages were used for the integrations in this study. The shortwave heat fluxes were applied with a single absorption coefficient of 1/17 m^{-1}. This is appropriate for the NWP flux but allows the climatological shortwave fluxes to penetrate deeper than is standard.

Both thermodynamic and dynamic sea ice processes are modelled in FOAM. The thermodynamic scheme is based upon the models of Semtner (1976) and for leads processes, Hibler (1979). The dynamic component is a simple advection scheme based on Bryan et al.

(1975), in which the ice thickness is advected with the top model level ocean currents. Further details of the sea ice formulation can be found in Cattle and Crossley (1995).

b. Observations and quality control

For many years temperature observations have been the most abundant direct measurements of the ocean available in near real-time. These data provide useful information on the large-scale ocean structure. Furthermore, the temperature field ia a prognostic model field and is an ocean model output of primary interest. For these reasons temperature data assimilation schemes have become well established and the FOAM assimilation scheme was initially developed to assimilate thermal profile and sea surface temperature (SST) observations. The FOAM data assimilation scheme has subsequently been enhanced to assimilate salinity observations and measurements from satellite radar altimeters, but these data are not included in the series of experiments described in this paper. Salinity observations are still rather sparsely distributed (although the prospect of mass deployment of PALACE floats (Davis 1998) may change this) and there are many issues relating to the altimeter data that are not the focus of this paper.

Sea surface temperature and sub-surface thermal profile observations that are received at the UKMO over the Global Telecommunications System (GTS) in near real-time. The majority of thermal profiles are measured by expendable bathythermographs (XBTs) from the Volunteer Observing Ship (VOS) program and thermistor chains from the TOGA-TAO moored buoy array in the tropical Pacific Ocean. Thermal profile observations are generally confined to the top 800 m of the ocean and are concentrated along shipping lanes and mooring lines in the tropical Pacific with large data sparse regions across the globe. The sparse distribution of thermal profile observations is highlighted by Fig. 1(a) which shows the global distribution for just one week in October 1995. In comparison, the temperature at the surface of the ocean is relatively well observed from both *in situ* and satellite observing platforms (Fig. 1b). SST data used in this study includes observations from ships, moored and drifting buoys and coarse resolution (2.5°) data from the AVHRR radiometers on board polar orbiting NOAA satellites. The geographical distribution of thermal profile observations used for assimilation and verification for the period of the integrations under consideration here is shown in Fig. 1(c,d) (see section 3 for a discussion).

Quality control of the observations is a vital part of any data assimilation system and as FOAM is intended to run each day the quality control is completely automated. The initial processing step selects observations in a specified area and time window, and the depths of those observations judged on the basis of their callsign to be XBTs are multiplied by a factor of 1.05 as they are widely accepted to have a shallow bias of about 5% (Hanawa and Yoritaka 1987). The main quality control step is based on a comparison with a "background field" which may be either climatology or an earlier analysis. In this study the background field is the Levitus (1994) monthly mean temperature climatology interpolated to the observation in space and time. Individual observations in a profile that differ from the background field by more than twice the climatological standard deviation (Levitus 1994) are flagged as having a gross error. If more than half of the observations in a profile fail the check then the whole profile is flagged and subsequently excluded in the assimilation. Approximately 5% of thermal profiles fail to pass this quality control step.

Profiles that do pass the check are averaged onto model levels using the following procedure:

i) Unflagged values in a profile are assigned to model layers and the mean of the difference between the observations and the background field is calculated for each layer. These differences are referred to here as ''observation increments''. The ratio of the expected error variance of the observation and the model field, as defined in (2.15), is set equal to 1 in layers containing one or more observations. As discussed in section 4, this somewhat arbitrary specification is perhaps one of the main weaknesses of the present system and one of our main priorities for improvement.

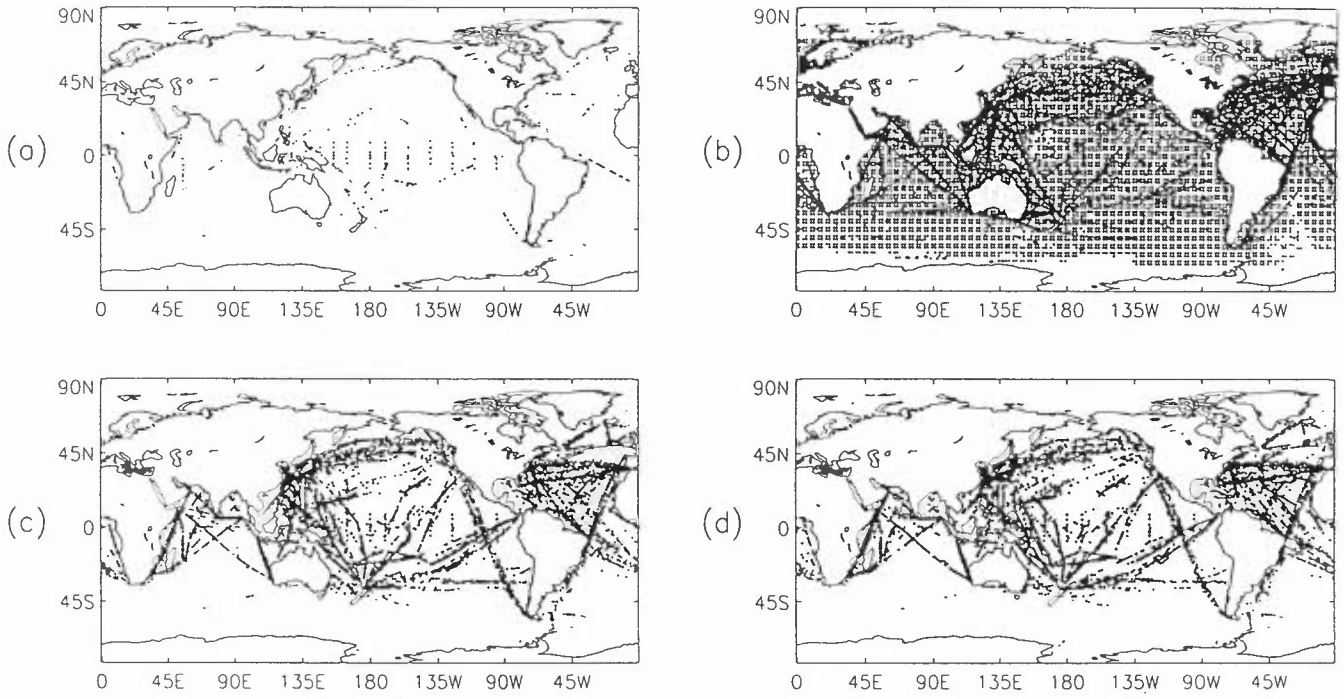

Figure 1. Locations of (a) thermal profile observations and (b) sea surface temperature observations for one week in October 1995. Also shown are locations of thermal profile observations for (c) assimilation, and (d) verification, in the twelve month period from May 1995 to April 1996.

ii) Model layers in which there are no observations are filled in by vertical interpolation of the observation increments and error ratios. This compensates for gaps in the observation profiles and also extends the influence of the data below the base of the original profiles. The interpolation uses vertical correlations between depths z_0 and z_1 of the form $exp(-20\ s^2)$ where $s = log(\ (z_0+a)\ /\ (z_1+a)\ )$ and $a = 25$ metres. The correlations are set to zero when $s^2 > 1.0$.

iii) The resulting observation increments are then added to the original background field to obtain a vertically coherent observation profile on model levels (i.e. mid-points of the model layers).

A sea surface temperature analysis is performed daily as part of the UKMO operational NWP suite to provide a lower boundary condition for the atmospheric model (Jones, 1991). FOAM uses the same SST quality control code as used by the NWP suite. The background check in this case is against the NWP suite SST analysis for the previous day rather than a climatology. Reports from moored and drifting buoys are received every hour and these observations are averaged over a 24 hour period to form "super-observations" which are subsequently used in the analysis. Further quality control checks are made during this stage to check the consistency of the platform. The "super-ob" fails if the standard deviation of reported values against the mean of the 24 hours of observations exceeds 0.5°C, the range of reported values over the 24 hours exceeds 0.5°C, or either latitude or longitude alters by more than 0.5 degrees during the reports.

c. Data assimilation scheme

The data assimilation component of FOAM is based on the iterative Analysis Correction method of Lorenc et al. (1991). Their technique is essentially a modified successive correction scheme which approximates Optimum Interpolation (OI). The notation in this section is exactly the same as in their paper.

1) The Analysis Correction method

Consider a system with N_x temperature grid points and N_y observations. Here, $\mathbf{y}_o$ is a column vector of temperature observations of length N_y and $\mathbf{x}_b$ is the model background field vector of length N_x. The aim of the data assimilation process is to find the optimum combination of observations and background field, taking into account the errors in both data sources, to produce a gridded analysis field $\mathbf{x}$. Assuming that the observational errors and model background field errors have Gaussian distributions, Lorenc (1986) shows that the optimum analysis field is the one for which the penalty function

$$J = [\mathbf{y}_o - \mathbf{k}(\mathbf{x})]^T(\mathbf{O}+\mathbf{F})^{-1}[\mathbf{y}_o - \mathbf{k}(\mathbf{x})] + (\mathbf{x}_b - \mathbf{x})^T\mathbf{B}^{-1}(\mathbf{x}_b - \mathbf{x}) \qquad (2.1)$$

is a minimum. Here $\mathbf{O}$ and $\mathbf{F}$ are the N_y x N_y observational error covariance matrices for the instrument errors and errors of representivity respectively, and $\mathbf{B}$ is the N_x x N_x background error covariance matrix. $\mathbf{K}$ is an interpolation operator from analysis grid points to observation locations; and the superscript T denotes the transpose. The matrices in Eq. (2.1) are large and an iterative technique is used to find the minimum of the penalty function and the resulting optimum analysis. The first and second partial derivatives of J are

$$\mathbf{J}' = -2\{\mathbf{K}^T(\mathbf{O}+\mathbf{F})^{-1}(\mathbf{y}_o - \mathbf{k}(\mathbf{x})) - \mathbf{B}^{-1}(\mathbf{x} - \mathbf{x}_b)\}, \qquad (2.2a)$$

$$\mathbf{J}'' = 2\{\mathbf{K}^T(\mathbf{O}+\mathbf{F})^{-1}\mathbf{K} + \mathbf{B}^{-1}\} \qquad (2.2b)$$

and the iterative solution is defined by

$$\mathbf{x}[u+1] - \mathbf{x}[u] = -\lambda(\mathbf{J}'')^{-1}\mathbf{J}' \qquad (2.3)$$

where the u^{th} estimate $\mathbf{x}[u]$ of the optimum analysis is used to derive the estimate $\mathbf{x}[u+1]$ and λ is a relaxation factor that controls the step size of the iteration. Substituting Eqs. (2.2) into Eq. (2.3) gives

$$\mathbf{x}[u+1] - \mathbf{x}[u] = \lambda(\mathbf{WK} + \mathbf{I})^{-1}\{\mathbf{W}[\mathbf{y}_o - \mathbf{k}(\mathbf{x}[u])] + (\mathbf{x}_b - \mathbf{x}[u])\} \qquad (2.4)$$

where

$$\mathbf{W} = \mathbf{B}\mathbf{K}^{T}(\mathbf{O}+\mathbf{F})^{-1} \qquad (2.5)$$

is an N_x x N_y matrix of "weights" - the weight relative to the background field given to each observation at each model grid point. The initial estimate $\mathbf{x}[0]$ is usually taken to be $\mathbf{x}_b$.

The N_x x N_x inverse matrix in Eq. (2.4) has to be approximated to find a solution. The rate of convergence depends strongly on the choice of approximation, though if convergence is achieved the OI solution is obtained whatever the approximation. In order to improve the rate of convergence of the algorithm when there are variations in observation density, Eq. (2.4) is re-written following the suggestion of Bratseth (1986) as:

$$\mathbf{x}[u+1] - \mathbf{x}[u] = \lambda\mathbf{W}(\mathbf{K}\mathbf{W} + \mathbf{I})^{-1}\{\mathbf{y}[u] - \mathbf{k}(\mathbf{x}[u])] \} \qquad (2.6a)$$

$$\mathbf{y}[u+1] - \mathbf{y}[u] = -\lambda(\mathbf{K}\mathbf{W} + \mathbf{I})^{-1}\{\mathbf{y}[u] - \mathbf{k}(\mathbf{x}[u])] \} \qquad (2.6b)$$

where the initial value for $\mathbf{y}[0]$ is the observation vector $\mathbf{y}_o$. Eq. (2.4) can be derived from Eqs. (2.6) by induction using the initial values $\mathbf{y}[0]=\mathbf{y}_o$ and $\mathbf{x}[0]=\mathbf{x}_b$ and the matrix identity

$$(\mathbf{W}\mathbf{K} + \mathbf{I})^{-1}\mathbf{W} = \mathbf{W}(\mathbf{K}\mathbf{W} + \mathbf{I})^{-1}. \qquad (2.7)$$

In the scheme described by Eqs. (2.6) both the model state and the modified observations converge towards the OI solution. The inverse matrix which is involved in Eqs. (2.6) will be termed $\tilde{\mathbf{Q}}$

$$\tilde{\mathbf{Q}} = (\mathbf{K}\mathbf{W} + \mathbf{I})^{-1}. \qquad (2.8)$$

Certain approximations are made to Eqs. (2.6) to form the Analysis Correction scheme. Firstly, $\tilde{\mathbf{Q}}$ is approximated by the reciprocal of the sum of weights at each observation point rather than the N_y x N_y matrix inverse of Eq. (2.8). The approximated $\tilde{\mathbf{Q}}$ is therefore a diagonal matrix of normalisation factors which takes into account the spatial density of observations. It can be shown that approximations to $\tilde{\mathbf{Q}}$ affect only the rate of convergence of the iteration, not the final limit.

Secondly in all the integrations presented in this paper, increments are not made to the observations (i.e. $\mathbf{y}[u]=\mathbf{y}_o$). The number of iterations and the choice of relaxation factor, λ, are thus crucial to the final analysis. They are chosen so that assimilation of a single observation would give results close to the OI solution. In data dense regions (where many observations influence each gridpoint) the resulting analyses are smoother than the OI solution and do not fit the observations as closely (Lorenc 1992). Some test assimilations which made increments to the thermal profile observations on the basis of Eq. (2.6b) and used larger relaxation factors did not give very different results.

Thirdly, the matrix $\mathbf{B}$ representing the background error covariance is modelled by a continuous function dependent on the distance between observation points and grid points, and on a correlation scale which varies with location and direction.

With these approximations Eqs. (2.6) become

$$\mathbf{x}[u+1] = \mathbf{x}[u] + \lambda \mathbf{W} \tilde{\mathbf{Q}} (\mathbf{y}_o - \mathbf{k}(\mathbf{x}[u])) \qquad (2.9)$$

Eq. (2.9) with **W** given by Eq. (2.5) and an approximation to the $\tilde{\mathbf{Q}}$ of Eq. (2.8) is the Analysis Correction scheme used in the FOAM data assimilation scheme.

2) Practical implementation

An iteration of the assimilation scheme is performed at each model timestep so that observation increments are nudged into the model over a period of time. The model is therefore able to adjust to the small changes imposed by the data at every timestep which takes into account prior knowledge that the ocean is slowly varying and removes the necessity for a separate adjustment step such as normal mode initialisation. The basic equation (2.9) for an analysis increment during one iteration at an individual grid point may be written as

$$\Delta x_m = \lambda \sum_i (\mu_{mi} \tilde{Q}_i \, R_i \, \Delta y_i) . \qquad (2.10)$$

The meaning of the terms in this equation are explained in the next few paragraphs (see Appendix 1 in Lorenc et al. (1991) for a derivation of Eq. (2.10)) . The model field at the mth grid point is denoted by x_m and Δx_m represents the analysis increment to the model field on a given iteration:

$$\Delta x_m = x_m[u+1] - x_m[u]. \qquad (2.11)$$

Denoting the model field interpolated to the ith observation as $k_i(\mathbf{x})$, Δy_i represents the observation increments:

$$\Delta y_i = y_i - k_i(\mathbf{x}) . \qquad (2.12)$$

The (estimated) forecast error covariance between a grid point m and observation point i, B_{mi}, is written as the product of the variance at the observation point and the correlation μ_{mi}

$$B_{mi} = B_{ii} \, \mu_{mi} \qquad (2.13)$$

The function μ is approximated as a second-order auto-regressive function:

$$\mu_{mi} = (1 + h_{mi}/s) \exp(- h_{mi}/s) \qquad (2.14)$$

where h_{mi} is the distance between observation *i* and grid point *m*, and *s* is the correlation scale. There is evidence to suggest that temperature variability close to the Equator has longer correlation scales in the east-west direction than in the north-south direction (e.g. Meyers et al. 1991). The correlation scale, *s*, in the assimilation scheme includes this anisotropy by defining

$$s = 300 + A \exp(- 0.5 \, t^2)$$
$$t = lat / 4.0$$

where *lat* is the grid point latitude in degrees, A = 300 km in the east-west direction and A = - 150 km in the north-south direction. This formulation results in an isotropic forecast

error correlation with a scale of 300 km away from the Equator. Close to the Equator, the correlation scale increases to a maximum of 600 km at the Equator in the east-west direction and decreases to a minimum of 150 km at the Equator in the north-south direction. As discussed in section 4, the determination of forecast error correlation scales is one aspect of the assimilation scheme that could be improved.

The observational error matrix **O + F** is taken to be diagonal. Only the ratio ε_i^2 of $(O+F)_{ii}$ to B_{ii} is required by the formulae;

$$\varepsilon_i^2 = (O + F)_{ii} \; / \; B_{ii} \quad . \qquad (2.15)$$

The normalisation factor $\tilde{Q}_i$ (which approximates the inverse matrix $\tilde{\mathbf{Q}}$) is given by a simple formulation using a weights function **D**, defined at each grid point as

$$D_m = \sum_i | \mu_{mi} | \; R_i \; / \; \varepsilon_i^2 \qquad (2.16)$$

where R_i [which also appears in (2.10)] is a time window weighting function depending on the difference between the analysis time and the observation validity time (described in more detail below). The summation in Eq. (2.16) is taken over all observations. $\tilde{Q}_i$ is then calculated by interpolating the gridpoint field **D** to the observation points with the formula

$$\tilde{Q}_i = \{ \varepsilon_i^2 (1 + k_i(\mathbf{D})) \}^{-1} \qquad (2.17)$$

A time window is defined for each observation type which specifies the length of time over which an observation is nudged into the model via the analysis iterations. Each observation is weighted in the analysis by the time window weighting function R_i, which takes the form of a symmetric linear ramp function with a maximum value of 1 at the observation validity time, falling off to zero either side of the specified time window. The asynopticity of observations is therefore taken into account in the assimilation scheme, giving a higher weight to an observation close to its validity time. A typical time window used for ocean temperature observations is five or ten days either side of the validity time.

As mentioned earlier, the relaxation factor λ is used to control the extent to which the analysis converges to the OI solution. λ has a value between 0 and 1 and controls directly the fraction of the increments introduced at each iteration step. It is defined so that the analysis of a single observation would converge to halfway between the observation and background values at the observation point for an error ratio $(O+F)_{ii} / B_{ii}$ equal to 1. The definition of λ takes account of the time window weighting function R_i which varies with time. The assimilation scheme is found not to be particularly sensitive to changes in the time window and relaxation factor.

The main computational cost in implementations of the Analysis Correction formulae are incurred in evaluating Eqs. (2.10) and (2.16). These formulae are both of the form

$$H_m = \sum_i \mu_{mi} F_i \qquad (2.18)$$

As this equation is linear it can be evaluated separately for various subsets of data and the resulting fields simply added together. The convolution of weights (Eq. 2.16) and increments (Eq. 2.10) from the observation points to the analysis grid has the form of a spatial grid-point recursive filter (Lorenc 1992). This filter is able to interpolate very dense data efficiently. The convolution is performed by three operations in sequence $\mathbf{SK^TA}$. $\mathbf{A}$ multiplies the values by an area weighting factor, $\mathbf{K}^T$ transfers the increments at the observation points to the analysis grid and $\mathbf{S}$ represents several passes of a recursive filter.

The recursive filter consists of a number of passes in both directions along each row and column of the two dimensional grid using the following formula

$$H_m = (1 - \alpha)\, G_m + \alpha\, H_{m-1} \qquad (2.19)$$

If data values are missing from the original field they are set to zero before filtering commences. A large number of passes of the left-to-right then right-to-left filters on a field $\mathbf{G}$ produce a field $\mathbf{H}$ which is a close approximation to the field which would be produced using a Gaussian filter. Two passes of the recursive filter approximates the second order auto-regressive function (Eq. 2.14) which is the form used in the assimilation scheme.

The computational efficiency of the ocean data assimilation system is important for the operational running of FOAM, and the assimilation scheme has been modified to run on a computer with massively parallel architecture (i.e. Cray T3E). The parallel version of the ocean model has a 1D domain decomposition so that each processor performs calculations for a latitude band on the model grid. Observations tend to be distributed irregularly across the model grid domain and there is a potential problem of computational load imbalance. However, the most computationally expensive part of the assimilation scheme is the recursive filter used in Eqs. (2.10) and (2.16) and by using a parallel version of the recursive filter, the assimilation scheme largely avoids this load imbalance. Because the spatial filter is only recursive in one dimension, 1D domain decompositions are used which alternate in the east-west and north-south directions as the filter changes from grid rows to grid columns. The computation time of the assimilation scheme is about 25% of the total when running the FOAM system.

3) Analysis groups

A separate analysis is performed for each data group (surface temperature, sub-surface temperature, salinity, surface height) at each iteration of the assimilation scheme. The analysis increments and derived balancing increments from each group are applied to the model fields sequentially. Specific details of the sea surface temperature and thermal profile analyses are as follows.

The first analysis is of the SST data and analysis increments are applied to the model temperature field in the surface layer and also to all levels in the mixed layer at each grid point. This is based on the assumption that the large scale mixed layer depth is fairly well defined by the model and thermal profile data assimilation. By definition the mixed layer has an almost constant temperature profile and a perfect error correlation is assumed between the surface temperature and the temperature down to the depth of mixing according to the Kraus-Turner scheme. There is no evidence of a long term drift in mixed layer depth using this technique. The time window over which the SST observations are nudged into the model

is set to five days (i.e. an observation influences the model five days either side of its validity time).

The thermal profile analysis is performed immediately after the SST analysis for all levels down to 1000 m depth. Increments in the thermal profile analysis are not applied to the model below 1000 m as there is very little data at this depth and increments are found to disrupt the barotropic streamfunction in the model. After the thermal profile analysis, balancing velocity increments are calculated from the thermal increments using hydrostatic balance and a modified geostrophic relation in which the Coriolis parameter, f, is increased near the equator. This is achieved by replacing the reciprocal of the Coriolis parameter by a function of the form

$$\frac{f}{f^2+a^2},$$

where $a = 3 \times 10^{-5}\ s^{-1}$. Only balancing baroclinic velocity increments are applied to the model at present and the impact of these velocity increments on the model is found to be small. A longer time window of ten days is used for nudging in the thermal profile data because the data distribution is relatively sparse.

d. A real-time ocean forecasting system

FOAM has been run operationally at the UKMO since August 1997 following a pre-operational trial during 1995 and 1996. FOAM is part of the UKMO Unified Model operational suite and performs a global analysis and forecast once per day. The ocean model is integrated forward 24 hours assimilating thermal data and continues into forecast mode for predictions a few days ahead. There are three main differences between the operational implementation of FOAM and the system used in the integrations described in this paper. Firstly, the ocean model is forced with 6 hourly mean surface fluxes from the UKMO operational NWP model throughout the period of assimilation and forecast. This enables variations in the mixed layer depth to be captured in the model due to rapidly changing wind stress patterns. Secondly, in the observation quality control check the background field is the FOAM analysis from 24 hours previously, rather than a climatology. Thirdly, in the real-time operational system only observations that have been received over the GTS by the analysis time can be included in the assimilation. When the FOAM system is run in delayed-mode all the observations are available and observations ahead of the analysis time within the specified time window can be assimilated.

3. Assessment of the data assimilation scheme

To assess the data assimilation component of FOAM a series of one year integrations with continuous data assimilation was performed. The period of integration from May 1995 to April 1996 was chosen to coincide with part of the pre-operational trial of FOAM. The integrations were started from rest from an initial state valid for 1 May 1995 in which the temperature and salinity fields are a linear interpolation of the April and May monthly mean Levitus (1994) temperature and salinity climatologies. Previous experiments with the ocean model run without data assimilation had shown that systematic errors grow rapidly in the first few months of integration starting from rest and continue to increase slowly over the following years. A one year period of integration was therefore considered to be adequate for assessing the data assimilation system and its effect on model systematic errors.

The performance of FOAM is assessed both qualitatively from geographical differences between gridded fields and quantitatively with statistics of differences from independent *in situ* thermal profile observations. The ocean is still relatively sparsely observed below the surface and there is a conflict between assimilating as many data as possible and holding data back for an independent verification of the resulting analyses. For the series of experiments in this paper, half of the available thermal profile observations are assimilated and the remaining half are used for verification. The two sets of data are not biased to any one region and have similar spatial distributions (Fig. 1c,d). For the independent verification, only those observations that pass the standard quality control check against the Levitus (1994) climatology are used. This means the same set of verification observations are used for all integrations but does result in a bias in favour of the climatological field in the verification. The period of integration also favoured climatology as it was not characterised by either an El Niño or a La Niña event. Root mean square temperature deviations are calculated for weekly analyses using observations valid within a 3.5 day time window either side of the analysis time.

a. Impact of data assimilation

To assess the impact of the data assimilation scheme four integrations of the model were performed; the first with no data assimilation (M), the second assimilated thermal profile observations only (A1), the third assimilated SST data in the surface layer and thermal profile observations (A2), and the fourth is similar to A2 but assimilates the SST data throughout the mixed layer (A3). All integrations were forced with monthly mean climatological surface fluxes.

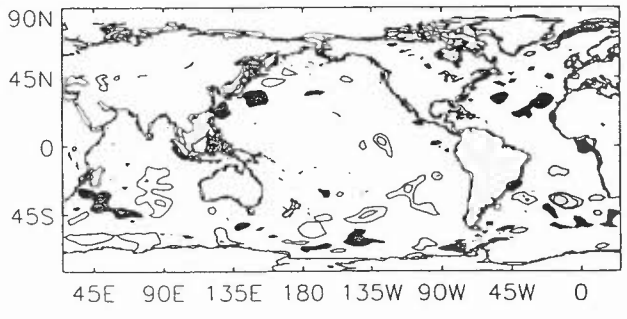

Figure 2. Sea surface temperature difference between the UKMO operational NWP analysis for 15 October 1995 and Levitus (1994) October climatology. Contours are plotted at ±1, 2 and 4°C. Cold anomalies below -1°C are lightly shaded. Warm anomalies greater than 1°C are heavily shaded.

Surface temperature anomalies for the four integrations are presented relative to the UKMO operational NWP SST analysis rather than the Levitus (1994) climatology. The NWP analysis uses the same set of SST observations as the model assimilation but is a statistically based analysis with no dynamical model. The NWP analysis therefore benefits from high spatial and temporal resolution satellite data, and may be expected to well represent daily variations in the SST field. This is in contrast to the monthly averaged Levitus climatology which uses *in situ* data alone. Intercomparisons of several SST analyses have shown consistency between different analyses, and have highlighted the importance of

satellite data in regions where *in situ* data is sparse (Folland et al. 1993). Figure 2 shows the differences between the NWP SST analysis and the Levitus climatology for October 1995. They are below 1°C over much of the globe but there are a number of isolated anomalies with magnitude greater than 1°C. In other years, departures from climatology can be very much larger, particularly in the tropical oceans in El Niño/La Niña years. Some of the anomalies seen in Fig. 2 will be due to inter-annual variations in the SST field, but others such as the ''bull's eye'' anomalies in the Southern Ocean do not persist from month to month in the Levitus climatology. Furthermore, no such ''bull's eye'' features are seen in month-to-month variations in the NWP SST analysis, which is based upon a much greater quantity of data in the Southern Hemisphere, and we therefore believe they are due to a lack of observations in these areas in the Levitus analyses.

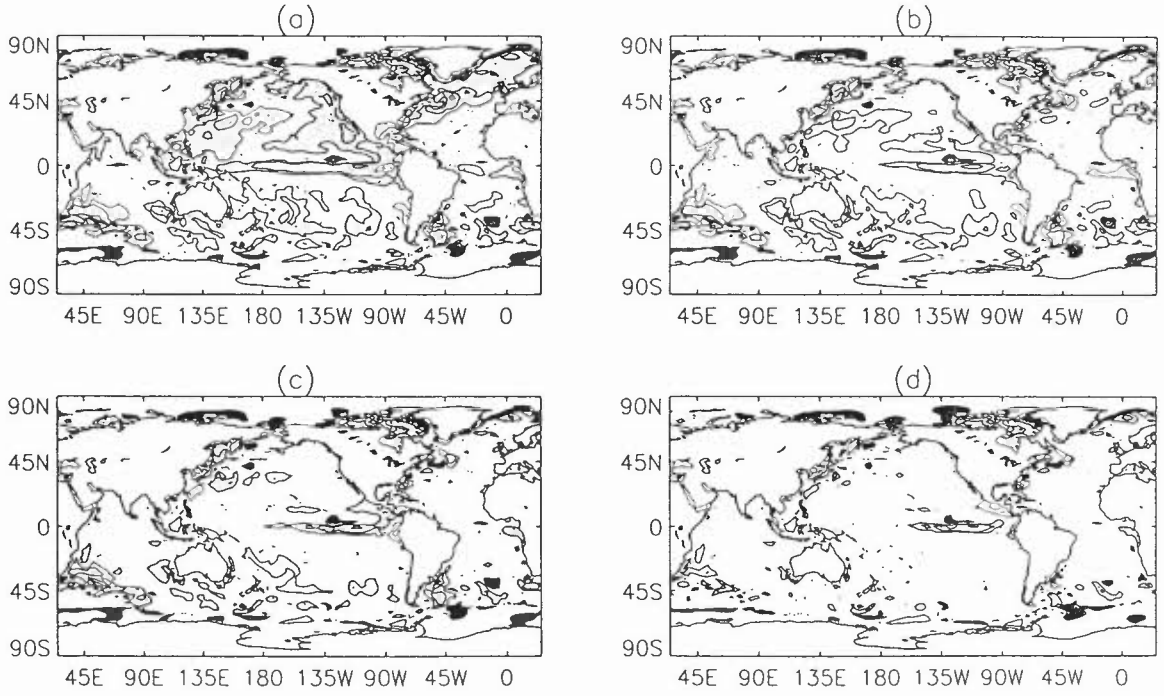

Figure 3. Sea surface temperature difference from the UKMO operational NWP analysis for 15 October 1995 after six months of integration for (a) model with no data assimilation, (b) model with thermal profile data assimilation, (c) model with thermal profile and sea surface temperature data assimilation in the surface layer, and (d) model with thermal profile and sea surface temperature data assimilation throughout the mixed layer. Contours and shading are the same as for Figure 2.

Surface temperature fields from all four integrations are compared against the NWP SST analysis in Figure 3. The drift away from climatology develops rapidly during the first few months of the model integration, M (Fig. 3a). Although the anomaly pattern does vary with time, a systematic bias is apparent in certain regions. The cold bias close to the Equator in the tropical Pacific Ocean is perhaps the most striking feature with a magnitude of over 3°C in the east. This is a common problem in ocean general circulation models (Stockdale et al. 1993) and the characteristics of the anomaly are found to be sensitive to the wind stresses

used to force the model, the formulation of the vertical mixing and the model resolution. Both the north and south Pacific Ocean basins also have a large-scale cold bias at the surface with a magnitude over 1°C. Other regions with significant anomalies include the western boundary currents and in particular the cold pool east of the Flemish Cap in the north-west Atlantic Ocean.

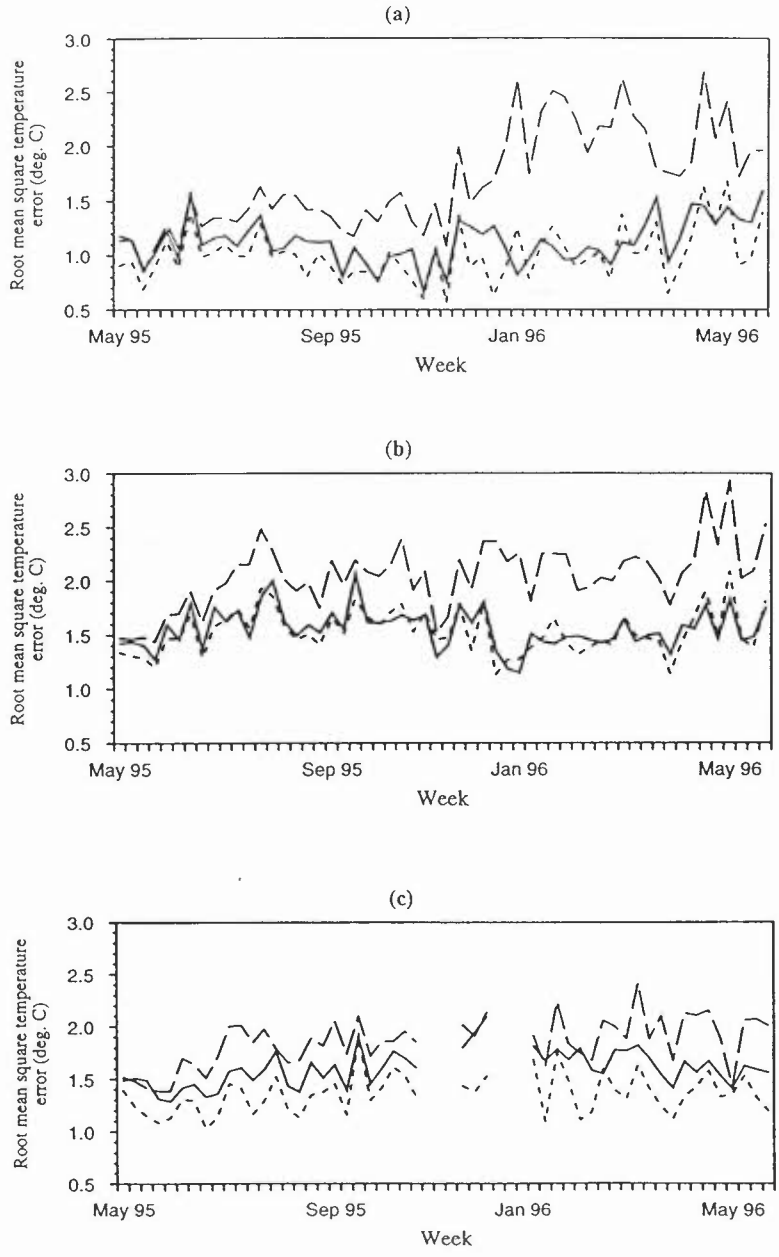

Figure 4. Time series of the temperature r.m.s. differences from observations for the Levitus (1994) climatology (solid line), the model integration M (dashed line) and the assimilation A3 (dotted line) for (a) the global ocean from 0 - 10 m, (b) the global ocean from 10 - 300 m and (c) the tropical Pacific Ocean (between 30°N and 30°S) from 0 - 300 m. The statistics are calculated every 7 days using observations that have not been assimilated into the model. The average number of observations per week used in the calculations is 200 for (a), 2000 for (b) and 700 for (c). The gaps in (b) correspond to weeks in which there were very few observations received in the tropical Pacific.

Assimilating thermal profile observations into the model (integration A1) reduces the surface temperature anomalies in the North and Equatorial Pacific, and North Atlantic basins (Fig. 3b). There is little change in the Southern Hemisphere oceans and parts of the north Pacific due to the lack of thermal profile observations in these areas (Fig. 1c). When SST data are additionally assimilated in the surface layer (integration A2), there is a further reduction in the surface temperature anomalies in all regions resulting from the increased coverage of the data (Fig. 3c). Assimilating the SST data throughout the mixed layer (integration A3) has an even greater impact and model anomalies are below 1°C in all but a few areas of the global ocean (Fig. 3d). Persistent anomalies greater than 1°C remain in integration A3 along the Equator in the eastern Pacific Ocean, in western boundary current regions and close to the ice edge. The assimilation scheme is unable to fully compensate for the model error along the Equator despite the good data coverage in this region. The western boundary currents are characterised by strong thermal gradients, and small displacements of the current can lead to significant temperature anomalies. Although some of the anomalies may be real features not captured in the statistically based NWP SST analysis, others may be related to deficiencies in the model or forcing fluxes. Near the ice edge differences between the assimilation and NWP SST analysis are related to the lack of data in these regions.

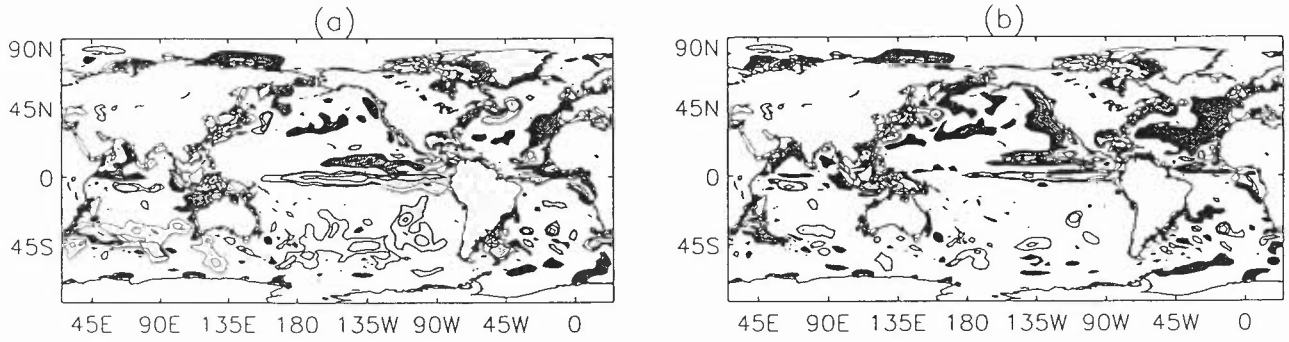

Figure 5. Potential temperature difference from Levitus (1994) climatology at 50m depth for October 1995 after six months of integration for (a) the model M integration and (b) the thermal profile and sea surface temperature data assimilation A3. Contours and shading are the same as for Figure 2.

A quantitative measure of the analysis error supports the qualitative assessment and highlights the temporal consistency of the results. Fig. 4 shows the root mean square error (r.m.s.e.) of the differences between the independent quality controlled thermal profile observations (Fig. 1d) and the model M, assimilation A3, and Levitus climate temperature fields for the year-long period of integration. Statistics are calculated for all observations in the depth ranges 0 - 10 m and 10 - 300 m in the global ocean, and 0 - 300 m in the tropical Pacific. These depth ranges were chosen in order to to obtain a large enough statistical sample. For the surface layer of the global ocean (Fig. 4a) the model temperature field has an average r.m.s.e. of 1.7°C during the year, considerably higher than the 1.1°C for the Levitus climatology. However, the assimilation is a significant improvement on the model and has the lowest overall temperature r.m.s.e. of 1.0°C. Below the surface, in the depth range 10 - 300 m (Fig. 4b), the average r.m.s.e. for the model, assimilation and climatology are all higher than in the surface layers. Again, the model has the highest mean r.m.s.e of 2.1°C whilst the Levitus climatology and the assimilation both have significantly lower mean r.m.s.e.s of 1.6°C and 1.5°C respectively. The model M r.m.s.e. is consistently worse than

climatology in all areas of the ocean. Although the assimilation r.m.s.e. is worse than climatology in certain regions such as western boundary currents, it significantly outperforms climatology in others, particularly the tropical Pacific Ocean (Fig. 4c).

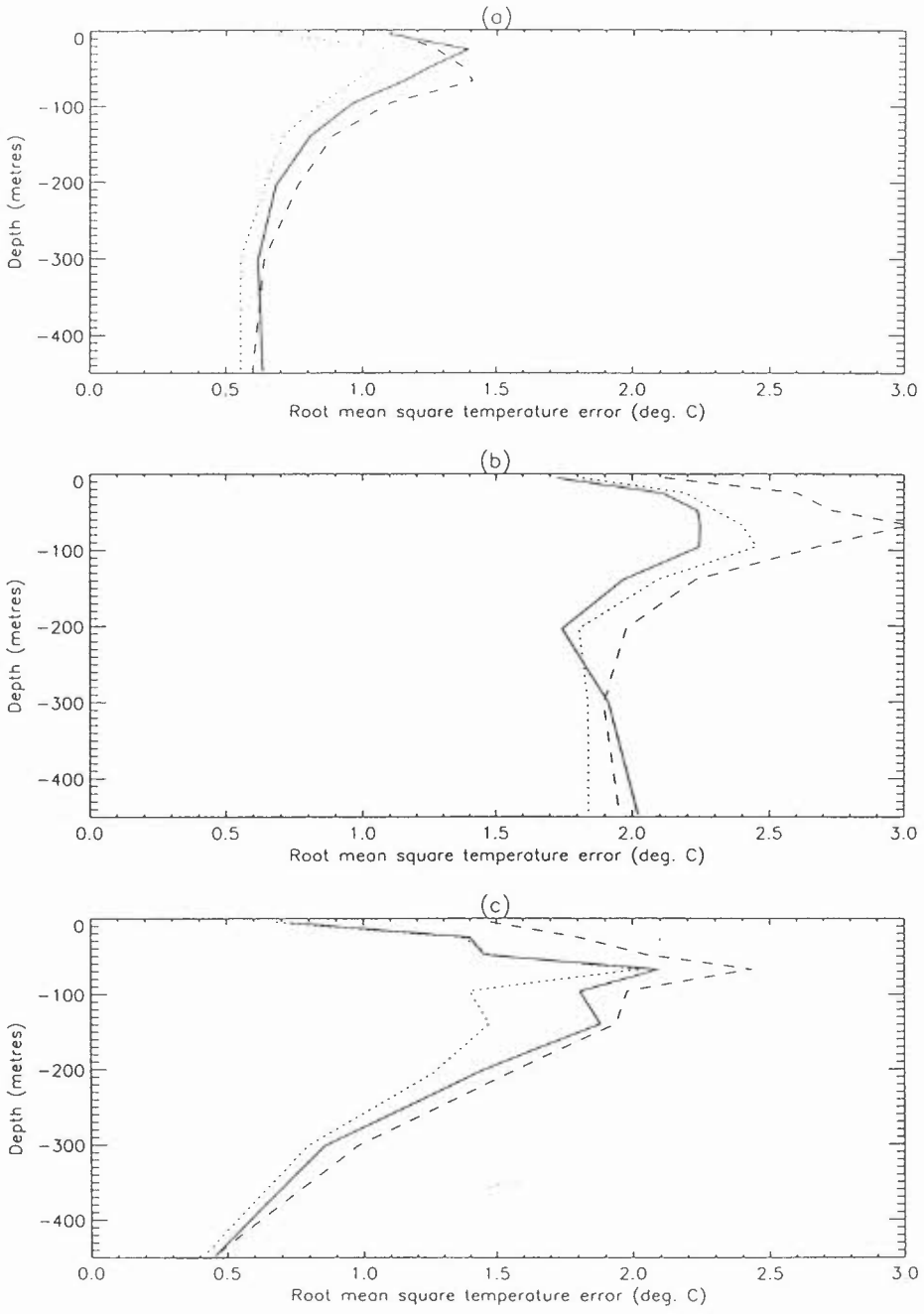

Figure 6. Variation with depth of the r.m.s. temperature differences from observations for the Levitus (1994) climatology (solid line), model M integration (dashed line) and assimilation A3 (dotted line) in (a) the eastern North Atlantic (15°N-60°N, 30°W-0°W) (b) western North Atlantic (15°N-60°N, 105°W-30°W), and (c) the tropical Pacific (15°S-15°N, 120°E-80°W). All statistics are calculated from independent observations in the one year period from May 1995 to April 1996. The average number of observations used in the calculation for each depth range is 500 for (a) and 1000 for (b) and 3000 for (c).

Figure 5 shows the model and assimilation potential temperature differences from the Levitus climatology at 50m depth. The most significant anomalies in the model integration M are similar in character to those at the surface except in the North Pacific and North Atlantic Oceans where the anomalies are of opposite sign (cf. Fig. 5a and Fig. 3a). As has already been suggested, some of the "bull's-eye" anomalies in the Southern Hemisphere also apparent at the surface (Fig. 2) are believed to be unrealistic features in the Levitus (1994) climatology. The assimilation A3 at 50m depth is generally closer to climatology than the model except in the North Atlantic and North Pacific oceans (Fig. 5b). To determine whether these are true anomalies, root mean square temperature differences from observations are calculated for each model layer in the top 450m. All observations during the year long period of integration were included so that a large enough observation sample was available. Results for the eastern and western North Atlantic are shown in Fig. 6(a,b). In the north-east region the assimilation is actually closer to the observations than both the climatology and the model, suggesting the cold anomaly at 50m depth is real (Fig 6a). The assimilation has the lowest r.m.s.e. at all model levels. In the north-west Atlantic the assimilation is significantly better than the model throughout the depth but has a higher r.m.s.e. than climatology in the top 250m (Fig 6b). This is related to the highly variable western boundary current region which is not resolved in a 1° model. Similar results are found for the eastern and western regions of the North Pacific ocean. Equivalent r.m.s.e. statistics for the top 450m in the tropical Pacific region (between 30°N and 30°S) show that the assimilation is not only better than the model at all depths but is a significant improvement on climatology below 70m depth (Fig. 6c).

b. Sensitivity to surface fluxes

The evolution of the model is sensitive to the particular characteristics of the atmospheric surface forcing fluxes and it is worthwhile investigating how the assimilation affects this sensitivity. Our knowledge of the forcing fluxes is known to be deficient in many areas and assimilating data can have a beneficial impact on the model by compensating for deficiencies in the forcing fluxes.

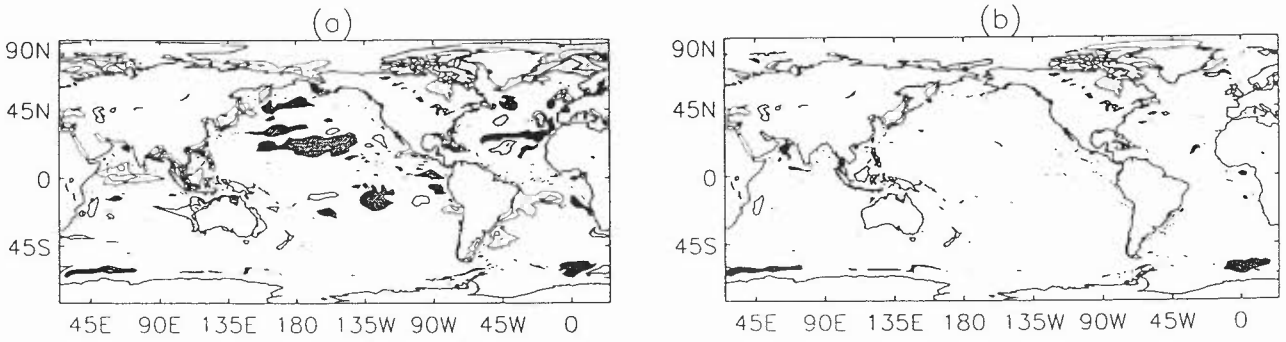

Figure 7. Potential temperature differences between integrations forced with UM and climatological heat fluxes (UM flux integration minus climate flux integration) at 50m depth for (a) the model with no data assimilation, and (b) the thermal profile and sea surface temperature assimilation. The fields are valid for October 1995 after six months of integration. Contours and shading are the same as for Figure 2.

To estimate typical uncertainties, two independent surface flux datasets are used to force the integrations; monthly mean surface fluxes from the UKMO operational NWP model (referred to as UM fluxes) and monthly mean climatological estimates (Oberhuber (1988) heat fluxes and Hellerman and Rosenstein (1983) wind stresses). The climatological fluxes are chosen as they are well established and have known "characteristics". A comparison against the Unified Model fluxes was chosen because the formulation of the two sets of fluxes is quite different and the differences between the fluxes are probably large enough to be representative of the actual errors in the fluxes. Only the effects of the heat and wind stress fluxes on the model temperature field are described as the precipitation/evaporation fluxes have a much smaller impact.

The heat and wind stress surface fluxes are assessed separately in two sets of four integrations; (i) model with all climate fluxes, (ii) model with climate fluxes but UM heat or wind stress fluxes, (iii) assimilation (as integration A3) with all climate fluxes, and (iv) assimilation with climate fluxes but UM heat or wind stress fluxes. Unfortunately UM fluxes were not available for August 1995 so they were replaced by climate fluxes for this month in the UM fluxes run, but this does not affect the qualitative aspect of the results. As the purpose of these experiments is to assess the differences in the model temperature field due to different fluxes, relaxation to a temperature climatology in the surface layer is not included in the integrations. The thermal relaxation term acts to reduce the impact of the fluxes (particularly the heat flux) on the model evolution.

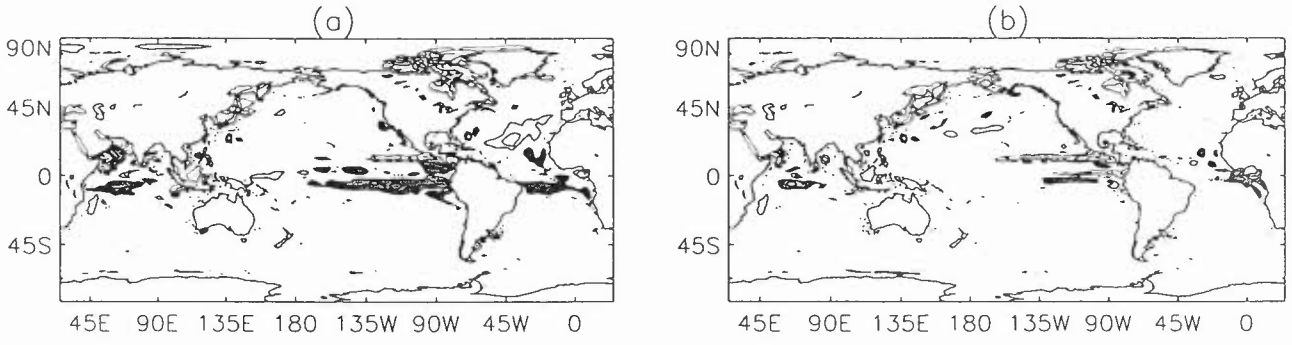

Figure 8. Same as Figure 7 except the integrations are forced with different wind stress fluxes.

Figures 7 and 8 show differences in the potential temperature field between two pairs of integrations of the model; one forced with climate fluxes and the other forced with the same climate fluxes but with the heat (Fig. 7) or windstress (Fig. 8) replaced with the UM derived fluxes. Only the potential temperature differences at 50m depth are shown as the characteristics are qualitatively similar at other depths but reduce in magnitude with depth. The impact of the different heat fluxes on the temperature field after only six months of model integration results in differences of over 1°C in many regions (Fig. 7a). The differences are significantly reduced by the thermal data assimilation scheme where there is a reasonably good distribution of surface temperature observations (Fig. 7b). Differences remain below 1°C over all depths, except near the ice edge where there are very few observations. However, some caution should be taken in extrapolating this result for the Southern Ocean to other months as the mixed layer is deeper than 50 metres there in October and the temperature in the mixed layer is determined by that at the surface where measurements are available. The impact of the different wind stress fluxes on the

temperature field (Fig. 8) is dominant in the equatorial regions, but there is also a 2°C difference in the North Atlantic subtropical gyre at 50m depth (Fig. 8a). The assimilation reduces the majority of these differences, but is not able to completely compensate for the effects of the different wind stresses close to the Equator and at 10°N in the eastern Pacific, eastern Atlantic and in parts of the Indian ocean (Fig. 8b). These are all areas that have a significant response to the wind stress forcing and the Hellerman-Rosenstein wind stresses are known to be much stronger than the UM fluxes in the equatorial Pacific and lighter than the UM fluxes in the southern hemisphere (Foreman et al. 1994, Jones 1996). It would certainly be worthwhile to investigate these results in more detail to attempt to draw more conclusions about errors in the fluxes by using the thermal analyses.

4. Discussion

It is apparent from Fig. 3 that one of the main roles of the assimilation of thermal data in the present FOAM system is to reduce the systematic drift of the model away from a realistic climatology. Fig. 3b shows that use of the thermal profile data alone reduces this drift significantly but not sufficiently in many areas (e.g. southern hemisphere and NW Pacific) to reach levels typical of differences from climatology. Almost all data assimilation schemes assume that the forecast fields are unbiased and while the systematic errors in the FOAM forecast fields are so large the philosophy of data assimilation, which is to combine best estimate forecasts with additional data, is in danger of being undermined. Thus it is important to reduce the magnitude of the errors in the fields produced without data assimilation.

Primitive equation models of 1° and 1/3° resolution are well known to be unable to simulate western boundary currents and their separation (Dengg et al. 1996) and at 1/3° resolution the path of the North Atlantic current to the north and east of the Flemish Cap depends a great deal on the model formulation (DYNAMO 1997). Some models of 1/10° resolution or better (Dukowicz and Smith 1994, Hurlburt and Hogan 1998) have a better representation of the mean current paths and also represent and (start to) resolve the very active mesoscale fronts and eddies in the ocean. Analysis and forecasting of these phenomena will be more akin to synoptic weather forecasting and estimation of initial conditions than the correction of model systematic error. As global models of very high resolution (1/10° or better) are computationally very expensive, and the group velocities in the ocean are fairly slow, our strategy is now to develop nested versions of the FOAM system which can be run at 1/3° and 1/10° resolution in selected areas.

As one of the main purposes of this paper is to document the FOAM data assimilation system it is appropriate to comment on what we perceive to be its main strengths and weaknesses and which aspects we are treating as priorities for improvement. The basic framework of Analysis Correction / optimal interpolation is not popular with most oceanographers who prefer to work on more ambitious 4D variational assimilation methods involving variants of the Kalman filter or model adjoints. We chose the simpler formulation for two main reasons. First we decided to gain experience with the practical problems of ocean data assimilation with a comparatively well established, well understood and uncomplicated scheme which could serve as a benchmark against which to judge more sophisticated schemes. Second we wanted to minimise the risks in code development and to ensure that we would not be severely restricted by the CPU time and space requirements of the assimilation scheme. Weather forecast centres, which have far larger resources for data

assimilation than our group, have found that well-tuned traditional schemes are quite competitive with initial implementations of 4D variational schemes.

The error variances and correlation scales presently used in the FOAM system have not been calculated from statistics of the errors in the system and do not depend much on geographical location. Some early tests with the assimilation system, reducing the correlation scales and observation error ratios, suggested that the results were not too sensitive to the specification of the error covariances. But now that the system has been used for more than 3 years we are able to estimate the error variances and (horizontal and vertical) forecast error correlations in selected regions. This development of statistically based and geographically varying error covariances is one of our two main priorities for improvement of the basic assimilation scheme. The other main priority is to assess which quality control checks would be most worthwhile, by examination of a large number of profiles, and to implement these checks. Our data preparation and quality control system is now part of that developed for numerical weather prediction so buddy checks and some station dependent checks are particularly easy for us to implement.

We have already experimented with the assimilation of altimeter data in our system (Forbes 1996) and in the past year data of sufficient quality for assimilation have become available within two days of real time. These data provide useful information on the state of El Niño and the most valuable information on the mesoscale circulation and are our highest priority for extension of the range of observation types which we use, though access to surface temperature data of higher resolution is also a priority. Our assimilation code is also able to assimilate salinity data and can be extended to assimilate velocity data, both of which will become available if ARGO (Argo Science Team 1998) comes to fruition. Finally we are experimenting with the use of SSM/I data for sea ice concentration.

5. Summary

This paper has documented the assimilation scheme used by the FOAM system and described a series of experiments which indicate the influence of data assimilation on the FOAM system and the uncertainties in the system due to lack of knowledge of the fluxes driving it.

The FOAM system has been run on a daily basis in pre-operational mode for nearly two years and has run in the Met. Office operational suite since August 1997. The present system includes global sea ice and primitive equation ocean models, is driven by six-hourly fluxes from the NWP system and assimilates surface temperature and thermal profile observations. The FOAM fields are, on average, closer to independent observations than the Levitus (1994) climatology in the top 200 metres of the NE Atlantic, NE Pacific and Equatorial [Pacific and Indian] Oceans. In the NW Atlantic and NW Pacific the FOAM fields largely match climatology. The data assimilation plays an important role in the FOAM system in reducing model drift (see Fig. 4). Assimilation of thermal profiles alone partly reduces this drift but surface data play an important role in reducing it further. Differences between two estimates of the surface fluxes lead to large differences in the thermal fields in the upper 50 metres after 6 months of integration without data assimilation (Fig. 7). These differences are substantially reduced by assimilation of the available data. Only in the tropical oceans do significant differences remain and these are driven by differences in the wind stresses.

Work is in progress to improve the FOAM system by improving the specification of the error variances and correlation scales, assimilating sea ice concentration data and altimeter data, and using higher resolution limited area models nested within the global model.

Acknowledgments

Many people have contributed to the development of the FOAM data assimilation system. We particularly wish to thank Howard Cattle, Steve Foreman, Andrew Cooper, Liam Gregorious and Grant Kelly for their support and assistance.

References

Argo Science Team, 1998: On the design and implementation of Argo - An initial plan for a global array of profiling floats. ICPO Report No. 21. GODAE Report No. 5. GODAE International Project Office, Melbourne, Australia, 32pp.

Behringer, D. W., M. Ji, and A. Leetma, 1998: An improved coupled model for ENSO prediction and implications for ocean initialization. Part I: The ocean data assimilation system. Mon. Wea. Rev., 126, 1013-1021.

Bell, M. J., 1998: Momentum fluxes in the Bryan-Cox ocean circulation model. J. Atmos. Oceanogr. Tech., 15, 6, 1401-1414.

Bratseth, A. M., 1986: Statistical interpolation by means of successive corrections. Tellus, 38A, 439-447.

Bryan, K., 1969: A numerical method for the study of the World Ocean. J. Comput. Phys., 4, 347 376.

Bryan, K., S. Manabe, and R. C. Pacanowski, 1975: A global ocean-atmosphere climate model. II. The oceanic circulation. J. Phys. Oceanogr., 5, 30-46.

Busalacchi A. J. 1997 Oceanic Observations. In: Data assimilation in meteorology and oceanography: theory and practice. Editor: Ghil, M. et al. J. Met. Soc. Japan, 21-44.

Cattle, H. and J. Crossley, 1995: Modelling Arctic climate change. Phil. Trans. R. Soc. Lond. A, 352, 201-213.

Clancy, R. M., J. M. Harding, K. D. Pollak, and P. May, 1992: Quantification of improvements in an operational global-scale ocean thermal analysis system. J. Atmos. Oceanogr. Tech., 9, 1, 55-66.

Cox, M. D., 1984: A primitive equation 3 dimensional model of the ocean. GFDL Ocean Group Tech. Rep. No. 1, Geophysical Fluid Dynamics Laboratory, 143 pp.

Cullen, M. J. P., 1993: The unified forecast/climate model. Meteorol. Mag., 122, 81-94.

Davey, M. K., S. Ineson, M. A. Balmaseda, 1994: Simulation and hindcasts of tropical Pacific Ocean interannual variability. Tellus, 46A, 433-447.

Davis, R. E., R. de Szoeke, and P. Niiler 1981: Variability in the upper ocean during MILE. Part II Modelling the mixed layer response. Deep-Sea Res., 28A, 1453-1475.

Davis, R. E. 1998: Autonomous floats in WOCE. International WOCE Newsletter, No.30, 3-6.

Dengg, J., A. Beckmann, and R. Gerdes, 1996: The Gulf Stream separation problem. In: The Warmwatersphere of the North Atlantic Ocean. pp 253-290. W. Krauss (Ed.) Gebrüder Borntraeger. Berlin.

Dombrowsky E., and P. de Mey, 1992: Continuous assimilation in an open domain of the northeast Atlantic. I. Methodology and application to Athena88. J Geophys. Res., 97, 9719-9731.

Dukowicz, J.K. and R.D. Smith, 1994: Implicit free-surface method for the Bryan-Cox-Semtner ocean model. J. Geophys. Res., 99, 7991-8014.

DYNAMO Group, 1997: Dynamics of North Atlantic Models: Simulation and assimilation with high resolution models. Institut fur Meereskunde, Kiel, Report No 294.

Esbensen, S. K., and Y. Kushnir, 1981: The heat budget if the global ocean: an atlas based on estimates from surface marine observations. Climate Research Institute, Oregon State Univ, Corvales, Report No. 69.

Folland, C. K., R. W. Reynolds, M. Gordon and D. E. Parker, 1993: A study of six operational sea surface temperature analyses. J. Climate, 6, 96-113.

Forbes, R. M., 1996: Initial results from experiments assimilating satellite altimeter sea surface height data into a tropical Pacific ocean model. Ocean Applications Technical Note No. 12. Available from the U.K. Meteorological Office.

Foreman, S. J., J. O. S. Alves, and N. P. J. Brooks, 1994: Assessment of surface fluxes from numerical weather prediction systems. Forecasting Research Division Technical Report 104. Available from the U.K. Meteorological Office.

Gerdes, R. C., C. Koberle, and J. Willebrand, 1991: The influence of numerical advection schemes on the results of ocean general circulation models. Climate Dyn., 5, 211-226.

Hanawa, K. and H. Yoritaka, 1987: Detection of systematic errors in XBT data and their correction. J. Ocean. Soc. Japan, 43, 68-76.

Haney, R. L., 1971: Surface thermal boundary conditions for ocean circulation models. J. Phys. Ocean. 1, 241-248.

Hayes, S. P., L. J. Mangum, J. Picaut, A. Sumi, and K. Takeuchi, 1991: TOGA-TAO: A moored buoy array for real-time measurements in the tropical Pacific Ocean. Bull. Amer. Meteor. Soc., 72, 339-347.

Hellerman, S., and M. Rosenstein, 1983: Normal monthly mean wind stress over the world ocean with error estimates. J. Phys. Oceanogr., 13, 1093 1104.

Hibler, W. D., 1979: A dynamic-thermodynamic sea ice model. J. Phys. Oceanogr., 9, 815-846.

Hurlburt, H. E. and P. J. Hogan, 1998: Impact of 1/8° to 1/64° resolution on Gulf Stream model-data comparisons in basin-scale subtropical Atlantic ocean models. Submitted to Deep Sea Research.

Jaeger, L., 1983: Montly mean patterns of global precipitation. pp129 140 in Streer Perrott, A., M. Beran, R. Ratcliffe (eds.) Variations in the global water budget. Dordrecht, Reidel.

Ji, M., A. Leetma, and J. Derber, 1995: An ocean analysis system for seasonal to interannual climate studies. Mon. Wea. Rev., 123, 460 481.

Johns, T. C., R. E. Carnel, J. F. Crossley, J. M. Gregory, J. F. B. Mitchell, C. A. Senior, S. F. Tett, R. A. Wood, 1997: The second Hadley Centre coupled ocean-atmosphere GCM: Model description, spinup and validation. Climate Dynamics, 13, 103-134.

Jones, C. G., 1996: Annual mean UKMO NWP surface fluxes for 1995 and 1994 compared with da Silva climatological fluxes. Ocean Applications Technical Note 8. Available from Meteorological Office.

Jones, C. P., 1991: The operational sea surface temperature analysis system. Short Range Forecasting Research Division Technical Note No. 67. Meteorological Office, U.K.

Kimoto, M., I. Yoshikawa, and M. Ishii, 1997: An ocean data assimilation system for climate monitoring. In: Data assimilation in meteorology and oceanography: theory and practice. Editor: Ghil, M. et al. J. Met. Soc. Japan, 471-487.

Kraus, E. B., and J. S. Turner, 1967: A one dimensional model of the seasonal thermocline. II. The general theory and its consequences. Tellus, 19, 98-106.

Large, W. G., J. C. McWilliams, and S. C. Doney 1994 Oceanic vertical mixing: a review and a model with a nonlocal boundary layer parametrization. Rev. Geophys., 31, 363-403.

Levitus, S., 1994: World Ocean Atlas 1994, CD-ROM Data Set Doc., Volume 3: Salinity and Volume 4: Temperature. Natl. Oceanic and Atmos. Admin., Washington D. C.

Lorenc, A. C., 1986: Analysis methods for numerical weather prediction. Quart. J. Roy. Meteor. Soc., 112, 1177-1194.

Lorenc, A. C., R. S. Bell, B. MacPherson, 1991: The Meteorological Office analysis correction data assimilaiton scheme. Quart. J. Roy. Meteor. Soc., 117, 59-89.

Lorenc, A. C., 1992: Iterative analysis using covariance functions filter. Quart. J. Roy. Meteor. Soc., 118, 569-591.

Meyers, G., G. H. Phillips, N. R. Smith, J. Sprintall, (1991). Space and time scales for optimum interpolation of temperature - Tropical Pacific Ocean. Progr. Oceanogr., 28, 189-219.

Oberhuber, J. M., 1988: An atlas based on the "COADS" data set: The budgets of heat buoyancy and turbulent kinetic energy at the surface of the global ocean. Report No. 15, Max Planck Institut fur Meteorologie, 20 pp.

Pacanowksi, R. C., and S. G. H. Philander, 1981: Parameterization of vertical mixing in numerical models of tropical oceans. J. Phys. Oceanogr., 11, 1443-1451.

Redi, M. H., 1982: Oceanic isopycnal mixing by coordinate transformation. J. Phys. Oceanogr., 12, 1154 1158.

Robinson, A. R., et al. 1996: Real-time operational forecasting on shipboard of the Iceland-Faeroe frontal variability. Bull. American Meteorological Society, 77, 243-259

Semtner, A. J., 1976: A model for the thermodynamic growth of sea ice in numerical investigatons of climate. J. Phys. Oceanogr., 6, 379-389.

Smedstad, O. M., D. N. Fox, H. E. Hurlburt, G. A. Jacobs, E. J. Metzger, J. L. Mitchell, 1997: Altimeter data assimilation into an 1/8° eddy resolving model of the Pacific ocean. In: Data assimilation in meteorology and oceanography: theory and practice. Editor: Ghil, M. et al. J. Met. Soc. Japan, 319-334.

Smith, N. R., 1995: An improved system for tropical ocean subsurface temperature analyses. J. Atmos. Oceanic Technol., 12, 850-870.

Stockdale, T., D. L. T. Anderson, M. Davey, O. Delecluse, A. Kattenberg, Y. Kitamur, M. Latif, T. Yamagata, 1993: Intercomparison of tropical ocean GCMs. WCRP, 79.

U. S. Naval Oceanographic Office and the U. S. Naval Ocean Research and Development Activity 1983 DBDB5 (Digital Bathymetric Data Base - 5 minute grid). U.S.N.O.O., Bay St. Louis.

World Climate Research Programme, 1996: Workshop on air-sea flux fields for forcing ocean models and validating GCMs. Editor: G. White.